Biochimica et Biophysica Acta, 778 (1984) 253–259
Elsevier

BBA 72292

SPECIFIC INTERACTION OF THE WATER TRANSPORT INHIBITOR, pCMBS, WITH BAND 3 IN RED BLOOD CELL MEMBRANES

MICHAEL F. LUKACOVIC *, A.S. VERKMAN **, JAMES A. DIX *** and A.K. SOLOMON

Biophysical Laboratory, Department of Physiology and Biophysics, Harvard Medical School, Boston, MA 02115 (U.S.A.)

(Received February 27th, 1984)

Key words: Water transport; Anion transport; Band 3; (Erythrocyte membrane)

The human red cell anion transport protein, band 3, contains six pCMBS (*p*-chloromercuribenzene sulfonate) reactive SH groups, five of which react with *N*-ethylmaleimide. We have carried out equilibrium binding experiments using *N*-ethylmaleimide-treated red cell ghosts and found that the sulfhydryl reactive water transport inhibitor, pCMBS, inhibits the binding to band 3 of the specific anion exchange inhibitor DBDS (4,4′-dibenzoamido-2,2′-disulfonic stilbene) in a non-competitive manner. Stopped-flow kinetic studies, in which DBDS is mixed with ghosts in the presence of pCMBS, show that pCMBS slows the DBDS induced conformational change in band 3. A non-competitive reaction scheme has been developed which incorporates the quantitative results of equilibrium and kinetic studies. The pCMBS effect on DBDS binding and kinetics is reversed with 5 mM cysteine suggesting a sulfhydryl bond is involved in pCMBS binding to band 3. These data suggest that pCMBS has a specific binding site on band 3, consistent with the hypothesis that band 3 mediates red cell water transport.

Introduction

Human red cell anion exchange is mediated by band 3, a 95 kDa glycoprotein which is present in about 550 000 non-covalent dimers per cell [1,2]. DBDS (4,4′-dibenzoamido-2,2′-disulfonic stilbene) binds specifically to band 3 [3,4] and is a potent inhibitor of anion exchange [3]. DBDS fluorescence increases by over two orders of magnitude when bound to band 3 [4,5].

Since DTNB (5,5′-dithiobis(2-nitrobenzoic acid)) had previously been found to inhibit red cell water transport and since DTNB migrated with band 3 when red cell membrane proteins were analyzed by gel electrophoresis, Brown et al. [6] suggested that band 3 played a role in water transport. pCMBS (*p*-chloromercuribenzene sulfonate), another sulfhydryl reagent, inhibits water [7], nonelectrolyte [7] and glucose transport [8] in red cells, but has no effect on red cell inorganic anion exchange.

We have previously reported [9] that there is an interaction between the water transport process and the anion exchange process, since DBDS binding to sites on band 3 is inhibited by pCMBS. The present study of the kinetics of the interaction shows that the inhibition is non-competitive and leads to a reaction scheme consistent with a possible role of band 3 in water transport.

* Present address: Procter and Gamble, Sharon Woods Technical Center, 11520 Reed Hartman Highway, Cincinnati, OH 45241, U.S.A.

** Present address: Brigham and Women's Hospital, Boston, MA 02115, U.S.A.

*** Present address: Department of Chemistry, SUNY, Binghamton, NY 13901, U.S.A.

Materials and Methods

Chemicals. DBDS was synthesized by the method of Kotaki et al. [10] and its purity was checked by thin-layer chromatography on Silica gel G in pyridine/acetic acid/water (10 : 1 : 40, v/v). pCMBS, cysteine, and *N*-ethylmaleimide were obtained from Sigma Chemical Co. (St. Louis, MO) and used without further purification.

Membrane preparation. Hemoglobin free unsealed red cell ghosts were prepared by a method similar to that of Dodge et al. [11]. Recently outdated blood was washed three times in 150 mM NaCl, 5 mM sodium phosphate (pH 8.0), hemolyzed at 0°C in 5 mM sodium phosphate (pH 8.0), washed four times in 5 mM sodium phosphate buffer, and then washed twice in 28.5 mM sodium citrate (pH 7.4). Ghosts were incubated with one volume of 2 mM *N*-ethylmaleimide for 1 h at 23°C and subsequently washed three times with 28.5 mM sodium citrate. Membrane protein concentration was assayed by the method of Lowry et al. [12].

N-Ethylmaleimide treatment. Band 3 contains six sulfhydryl groups [13,14]. Five of these are located on the cytoplasmic side of the membrane and react with *N*-ethylmaleimide [15]. The sixth, which is located in the 17 kDa membrane bound fragment of band 3 between the trypsin and the chymotrypsin cuts [16], does not react with *N*-ethylmaleimide [17] but does react with pCMBS [9]. Rao [18] has shown that reaction of the cytoplasmic sulfhydryl groups with *N*-ethylmaleimide blocks subsequent reaction with pCMBS. She found that *N*-ethylmaleimide uptake in red cell ghosts saturated at 0.2 to 0.5 mM *N*-ethylmaleimide for 1 h incubation at 37°C. All of our experiments have been done with *N*-ethylmaleimide treated ghosts that have been incubated with one volume of 2 mM *N*-ethylmaleimide for 1 h at 23°C and subsequently washed three times with 28.5 mM citrate. Since we have used a higher *N*-ethylmaleimide concentration and a lower temperature than Rao, we have carried out control experiments to see whether longer times of incubation or higher temperatures had any effect in our system. Neither extending the incubation time to 2 h at 23°C or raising the temperature for a 1 h incubation to 37°C caused any change in the effect of pCMBS on DBDS fluorescence enhancement. This indicates that the pCMBS effects reported in this paper are not to be attributed to the cytoplasmic SH groups.

Binding studies. Equilibrium binding of DBDS to *N*-ethylmaleimide treated red cell ghost membranes was determined at 25°C by the fluorescence enhancement technique described by Verkman et al. [4]. The fluorescence of a ghost solution (0.04 mg/ml protein) was measured (excitation 350 nm, emission 427 nm) in a fluorescence spectrophotometer (MFP-2A, Perkin Elmer Co., Norwalk, CT). Aliquots of DBDS were added to the ghost solution to give DBDS concentrations ranging from 0.02 μM to 10 μM. The measured fluorescence intensity was assumed to be proportional to the concentration of bound DBDS after corrections were made for inner filter effects, scattering and fluorescence of free DBDS.

Stopped-flow studies were performed as described elsewhere [4] using a dual-jet mixing chamber. 1.0 ml of a 0.04 mg/ml ghost protein solution was rapidly mixed with 1.0 ml of a DBDS solution; the time course of DBDS binding to ghosts was determined by measuring DBDS fluorescence. In studies of pCMBS effects, an equal concentration of pCMBS was present in both ghost and DBDS solutions. Fluorescence time course data were stored on a waveform recorder (Biomation model 805, Cupertino, CA) and transferred to a computer (PDP 11/34, Digital Equipment Corp., Maynard, MA) for numerical analysis.

Results

In 28.5 mM sodium citrate, DBDS first binds [4] to one monomer of a band 3 dimer with a dissociation constant of 3 μM. DBDS then induces a slow conformational change (2.5–4 s^{-1}) which both locks DBDS into a high affinity site ($\approx$ 0.065 μM) and alters the affinity for binding of DBDS to the second monomer according to the reaction scheme below. The total number of sites of both classes is about $1.2 \cdot 10^6$ sites/red cell.

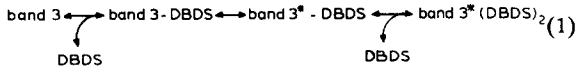

(1)

Equilibrium fluorescence titrations for DBDS binding to ghosts were performed and analyzed as

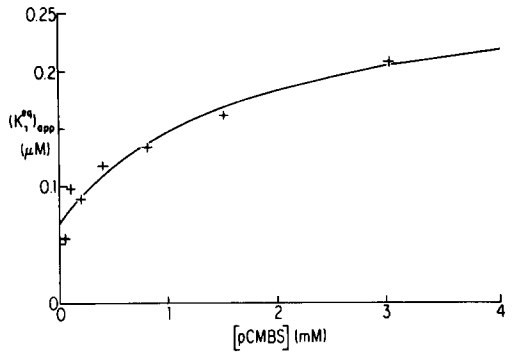

Fig. 1. Effect of pCMBS on DBDS binding to ghosts. The apparent dissociation constant for DBDS binding to *N*-ethylmaleimide-treated ghosts, $(K_1^{eq})_{app}$, was measured by the fluorescence enhancement binding technique [4] at several pCMBS concentrations. Each data point represents results of a fluorescence titration in which the fluorescence of a solution containing ghosts, pCMBS and 15 DBDS concentrations is measured. Data were fitted to a rectangular hyperbola of the form $(K_1^{eq})_{app} = \alpha[\text{pCMBS}]/[\text{pCMBS} = K_{1/2}) + \beta$, with $K_{1/2} = 1.7 \pm 0.3$ mM and $\alpha = 212$ nM, $\beta = 70$ nM.

previously described [4]. In the presence of pCMBS, there were two classes of binding sites for DBDS to band 3; plots of corrected fluorescence intensity, F, (proportional to bound DBDS) as a function of [DBDS] were fitted to a two site sequential binding model with dissociation constants *, $(K_1^{eq})_{app}$ and $(K_2^{eq})_{app}$.

$$F = A\frac{(K_2^{eq})_{app}[\text{DBDS}]/2 + [\text{DBDS}]^2}{(K_1^{eq})_{app}(K_2^{eq})_{app} + (K_2^{eq})_{app}[\text{DBDS}] + [\text{DBDS}]^2} \quad (2)$$

where A is a fitted parameter. While $(K_1^{eq})_{app}$ can be determined well from the data, $(K_2^{eq})_{app}$ is not well determined since $(K_2^{eq})_{app}$ is comparable to the maximum DBDS concentrations studied (see footnote for notation).

Fig. 1 shows a plot of $(K_1^{eq})_{app}$ as a function of [pCMBS]. The data show that pCMBS decreases the affinity of DBDS binding to band 3. Since $(K_1^{eq})_{app}$ saturates at high [pCMBS], DBDS has a finite dissociation constant even as [pCMBS] becomes infinite. Therefore, both DBDS and pCMBS can bind simultaneously to interacting sites on the red cell ghost membrane. In general, a curvilinear relation between $(K_1^{eq})_{app}$ and inhibitor concentration is taken to indicate the presence of a noncompetitive interaction (Segel [19]).

If NaCl replaces a significant amount of citrate, the binding mechanism is altered and only one class of DBDS binding sites on band 3 is observed with $1.2 \cdot 10^6$ sites/red cell (Dix, J.A., Verkman, A.S. and Solomon, A.K., unpublished data). Under these conditions, the binding mechanism consists of a fast bimolecular association (dissociation constant, K_1) followed by a slower conformational change (forward rate constant, k_2, reverse rate constant, k_{-2}),

$$\text{band 3} \underset{\text{DBDS}}{\overset{K_1}{\rightleftharpoons}} \text{band 3-DBDS} \underset{k_{-2}}{\overset{k_2}{\rightleftharpoons}} \text{band 3*-DBDS} \quad (3) \qquad (3)$$

The experimentally determined equilibrium dissociation constant, K_1^{eq}, for DBDS binding to band 3 is related to K_1, k_2 and k_{-2} in Eqn. 3 by

$$K_1^{eq} = K_1/(1 + k_2/k_{-2}) \quad (4)$$

where

$$K_1^{eq} = \frac{[\text{DBDS}][\text{band 3}]}{[\text{band 3-DBDS}] + [\text{band 3*-DBDS}]}$$

$$K_1 = \frac{[\text{DBDS}][\text{band 3}]}{[\text{band 3-DBDS}]}; \quad k_2/k_{-2} = \frac{[\text{band 3*-DBDS}]}{[\text{band 3-DBDS}]} \quad (5)$$

Since K_2^{eq} is poorly determined in the presence of pCMBS, we have analyzed the pCMBS effect using only the reaction steps given in equation 3 and not taking any account of possible pCMBS effects on $(K_2^{eq})_{app}$. As will be shown, a self-consistent reaction model for the effect of pCMBS can be generated without the inclusion of any steps beyond those given in Eqn. 3.

Eqn. 4 indicates that K_1^{eq} is composed of the

* The notation for the equilibrium binding (dissociation) constants used in this paper is:
K_1, dissociation constant for the first step of the DBDS binding mechanism in Eqn. 3.
K_1^{eq}, K_2^{eq}, experimentally determined dissociation equilibrium constants for DBDS binding in the absence of pCMBS.
$(K_1)_{app}$, apparent dissociation constant for the first bimolecular step in the presence of pCMBS.
$(K_1^{eq})_{app}$, $(K_2^{eq})_{app}$, experimentally determined dissociation constants for DBDS binding in the presence of pCMBS.
K_I, dissociation constant for pCMBS binding to band 3.
The notation for the rate constants is:
k_2, k_{-2}, rate constants for the second step in Eqn. 3.
k_2^{app}, k_{-2}^{app}, apparent rate constants for the second step in the presence of pCMBS.

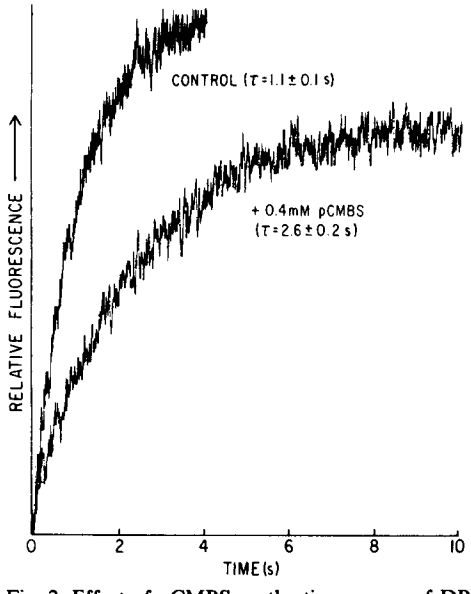

Fig. 2. Effect of pCMBS on the time-course of DBDS binding to ghosts in a stopped-flow experiment. 1 μM DBDS was mixed with *N*-ethylmaleimide-treated unsealed ghosts (0.04 mg/ml ghost protein) in 28.5 mM sodium citrate (pH 7.4), 23°C in the presence and absence of 0.4 mM pCMBS. 90° fluorescence was measured at an excitation wavelength of 358 nm and emission wavelength > 420 nm.

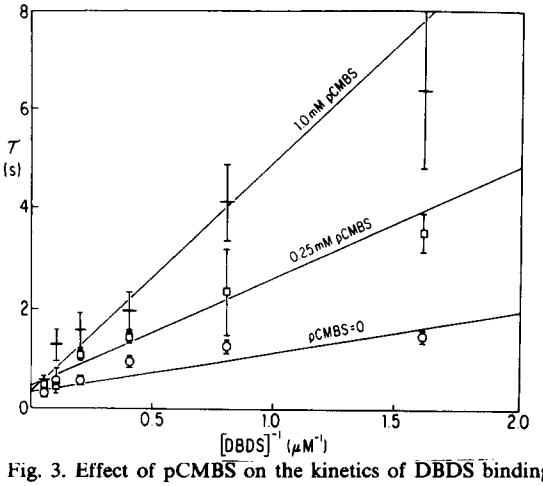

Fig. 3. Effect of pCMBS on the kinetics of DBDS binding to ghosts. Each point represents the average of three experiments on *N*-ethylmaleimide-treated ghosts; error bars are one standard deviation. Lines were fitted to data for each pCMBS concentration by weighted linear least squares with results given in Table I. [pCMBS] = 0 mM, (○, $r^2 = 0.93$); 0.25 mM (□, $r^2 = 0.96$); 1.0 mM (+, $r^2 = 0.96$).

dissociation constant K_1 and rate constants k_2 and k_{-2}. In order to define the detailed effects of pCMBS on these three parameters, stopped-flow experiments were carried out. Fig. 2 shows the time-course of increasing fluorescence observed when DBDS is mixed rapidly with band 3 in red cell ghosts. Increasing fluorescence corresponds to formation of the band 3*-DBDS complex [4]. Addition of 0.4 mM pCMBS decreases the total amplitude and increases the exponential time constant for the process. In the absence of pCMBS, the exponential time constant, τ, is related to the parameters K_1, k_2 and k_{-2} by the following equation which is exact for the mechanism given in Eqn. 3 (when [DBDS] $\gg$ [band 3]) and approximate for the sequential binding mechanism in Eqn. 1 [20],

$$\tau = \left(k_{-2} + k_2 \frac{[\text{DBDS}]}{[\text{DBDS}] + K_1} \right)^{-1} \tag{6}$$

The effect of pCMBS on the process can be examined by assuming that Eqn. 6 is still approximately valid in the presence of pCMBS and treating K_1, k_2 and k_{-2} as functions of [pCMBS]. By exploring the details of this dependence, it is possible to determine how the reaction scheme in Eqn. 3 must be modified to take into account the detailed pCMBS interactions with band 3.

Fig. 3 shows a plot of τ as a function of $[\text{DBDS}]^{-1}$ for [pCMBS] = 0, 0.25 and 1.0 mM. The data for each pCMBS concentration fit a straight line reasonably well ($r^2 = 0.93$–0.96; see Fig. 3 legend), suggesting that k_{-2} may be neglected which reduces Eqn. 6 to:

$$\tau = \frac{(K_1)_{\text{app}}}{k_2^{\text{app}}} \frac{1}{[\text{DBDS}]} + \frac{1}{k_2^{\text{app}}} \tag{7}$$

Table I gives values for $(K_1)_{\text{app}}$ and k_2^{app} determined from the slopes and intercepts of the lines for the three pCMBS concentrations in Fig. 3. It is clear that $(K_1)_{\text{app}}$ changes with pCMBS, while k_2^{app} does not change significantly in the range [pCMBS] = 0 to 1 mM.

In order to define the dependence of $(K_1)_{\text{app}}$ on pCMBS more fully, time-courses were obtained at 0.5 μM DBDS, which is of the same magnitude as $(K_1)_{\text{app}}$. Since Table I shows that k_2^{app} does not change with [pCMBS], $(K_1)_{\text{app}}$ can be related to

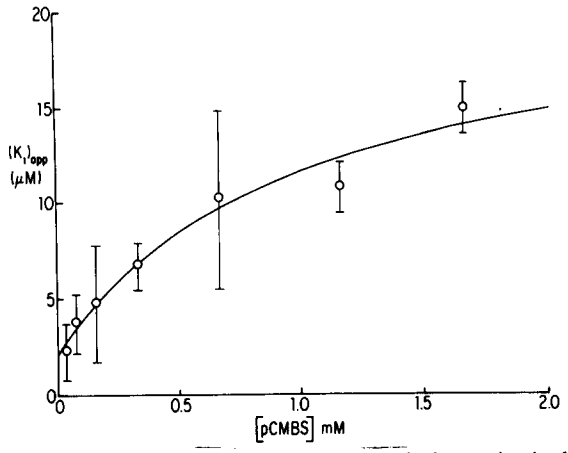

Fig. 4. Effect of pCMBS on $(K_1)_{app}$. Each data point is the average of three determinations on *N*-ethylmaleimide-treated ghosts; error bars are one standard deviation. The data were fitted by non-linear least squares to the rectangular hyperbola, $(K_1)_{app} = D([pCMBS]/(E + [pCMBS])) + G$, with $D = 19 \pm 3$ μM, $E = 0.9 \pm 0.3$ mM and $G = 2 \pm 1$ μM.

the observed value of τ at 0.5 μM DBDS, $\tau_{0.5}$, using Eqn. 6,

$$(K_1)_{app} = [DBDS]\left(\frac{k_2^{app}\tau_{0.5}}{1 - k_{-2}^{app}\tau_{0.5}} - 1\right) \quad (8)$$

The value for k_{-2}^{app} ($k_{-2}^{app} = 0.034$ s^{-1}) was determined by an iterative process in which we varied k_{-2}^{app} until, at infinite pCMBS concentration, $(K_1^{eq})_{app}$ was made to equal the limiting value of $(K_1^{eq})_{app}$ as calculated from the data in Fig. 1 by an equation analogous to eq. 4.

$$(K_1^{eq})_{app_{(pCMBS \to \infty)}} = K_1'/(1 + k_2'/k_{-2}') \quad (9)$$

This method assumes that k_{-2}^{app} is independent of pCMBS concentration. Comparison of the shape of the curves for the observed data (Fig. 1, $[pCMBS]_{1/2} = 1.7 \pm 0.3$] with that of the calculated curve (Fig. 4, $[pCMBS]_{1/2} = 0.9 \pm 0.3$) shows fair agreement, consistent with the independence of both k_2^{app} and k_{-2}^{app} of pCMBS concentration.

Fig. 4 shows values for $(K_1)_{app}$ (calculated from $\tau_{0.5}$ for various pCMBS concentrations using Eqn. 8) as a function of pCMBS. It is clear that $(K_1)_{app}$ saturates; a fit of $(K_1)_{app}$ vs. [pCMBS] to a rectangular hyperbola as described in the legend of Fig. 4 gives a saturating $(K_1)_{app}$ value of 21 ± 4 μM as $[pCMBS] \to \infty$.

If pCMBS and DBDS were to compete for a single binding site on band 3, a plot of $(K_1)_{app}$ vs. [pCMBS] would be linear, indicating that all DBDS binding could be abolished at sufficiently high concentrations of pCMBS. This is not the case. A curved plot of $(K_1)_{app}$ vs. [pCMBS], with saturating behavior at high [pCMBS] indicates that DBDS binding can occur even at infinite [pCMBS] which is not consistent with competition for a single binding site. This means that neither the reaction scheme given in Eqn. 1, or the simpler one given in Eqn. 3 is satisfactory. Instead a complete solution requires inclusion of two distinct sites on band 3, one for DBDS and another for pCMBS. The simplest non-competitive scheme for DBDS and pCMBS binding to band 3 is given by

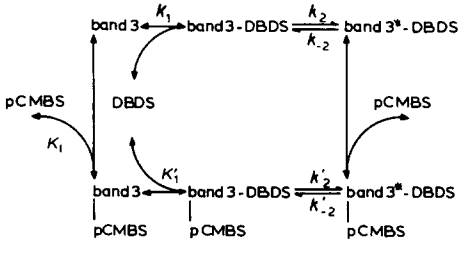

(10)

TABLE I

EFFECT OF pCMBS ON KINETICS OF DBDS BINDING TO GHOSTS

Results were obtained from a weighted linear least-squares fit to the data in Fig. 3. Experiments were performed in 28.5 mM sodium citrate (pH 7.4) at 23°C. The present results for k_2 and K_1 at [pCMBS] = 0 mM differ somewhat from our previous [4] results ($k_2 = 4$ s^{-1}; $K_1 = 3$ μM) probably because of small differences in the DBDS synthesis and purity; the preparations were synthesized by different individuals in different laboratories.

pCMBS (mM)	Slope (s·μM)	Intercept (s)	$k_2^{app} = 1/\text{intercept}$ (s^{-1})	$(K_1)_{app}$ = slope/intercept (μM)
0	0.78 ± 0.15	0.40 ± 0.10	2.5	1.95
0.25	2.32 ± 0.33	0.45 ± 0.09	2.2	5.2
1.0	4.33 ± 0.59	0.40 ± 0.08	2.5	10.8

Although the model given in Eqn. 10 contains four more parameters than are required for the model in Eqn. 3, it is possible to evaluate the additional equilibrium constants K_1 and K_1' and the rate constants k_2' and k'_{-2} by using data from Figs. 1, 3 and 4. The three parameters in the top limb of Eqn. 10 are those given in Table I in the absence of pCMBS ($K_1 = 1.95$ μM; $k_2 = 2.5$ s^{-1} and $k_{-2} = 0.034$ s^{-1}) obtained as described above. The parameters in the bottom row of Eqn. 10 are determined at infinite [pCMBS]; $K_1' = 21$ μM from the limiting value of $(K_1)_{app}$ as computed from the curve in Fig. 4. Since k_2^{app} is independent of pCMBS concentrations, $k'_2 = k_2$ from Table I. As discussed above k_{-2}^{app} is also considered independent of pCMBS concentration, so $k'_{-2} = 0.034$ s^{-1}.

The value for K_I is determined from the dependence of (K_1^{eq}) on [pCMBS],

$$(K_1^{eq})_{app} = K_1\left(\frac{1+[pCMBS]/K_I}{(1+k_2/k_{-2})+[pCMBS](1+k_2'/k'_{-2})K_1/K_1'K_1}\right) \quad (11)$$

Fig. 1 shows $(K_1^{eq})_{app}$ is half way between its value at 0 (70 nM) and infinite (280 nM)[pCMBS] at approx. 1.7 mM. Using known values for K_1, K_1', k_2, k_2', k_{-2} and k'_{-2}, [pCMBS] = 1.7 mM and $(K_1^{eq}) = 1/2$ (70 + 280) nM, Eqn. 11 predicts K_I ~ 0.11 mM.

A useful way to check the internal self consistency of the model in Eqn. 10 is using the additional observation, in Fig. 4, that $(K_1)_{app}$ reaches half-saturation at [pCMBS] ~ 0.9 mM. This observation has not been used to evaluate any of the model parameters so far and therefore serves as an independent, redundant test of self-consistency. $(K_1)_{app}$ can be expressed as a function of [pCMBS], K_1, K_1', and K_I

$$(K_1)_{app} = \frac{K_1(1+[pCMBS]/K_I)}{1+\frac{[pCMBS]K_1}{K_IK_1'}} \quad (12)$$

The value of [pCMBS] at half maximum $(K_1)_{app}$, $(K_1 + K_1')/2$, can be estimated using $K_1 = 1.95$ μM, $K_1' = 21$ μM, $K_I = 0.11$ mM and Eqn. 12. The [pCMBS] at half maximum $(K_1)_{app}$ is approx. 1.2 mM, in reasonable agreement with the observed value of approx. 0.9 mM from Fig. 4.

Discussion

The conclusion that pCMBS binding is not competitive with DBDS binding is based on the observations that maximal concentrations of pCMBS do not entirely inhibit the DBDS interaction with band 3. The major effect of pCMBS, as indicated in Fig. 5, appears to be on $(K_1)_{app}$ which suggests that pCMBS bound at one site specifically modifies the structure for the initial DBDS binding site and not the activation energy barriers for the DBDS conformational change. This may mean that pCMBS shares a site spatially near the initial DBDS site on band 3, but at some distance from the final DBDS site on band 3 which is occupied once the band 3-DBDS conformational change has occurred. This might happen if, as suggested by Solomon et al. [9], the pCMBS and DBDS sites are located near the external membrane surface on the inside of an aqueous pore, and only DBDS can undergo an 'internalization'; this would correspond to a conformational change which removes DBDS from the vicinity of the pCMBS site.

Water transport in the human red cell is inhibited by the organic mercurials, pCMBS and *p*-chloromercuribenzoic acid (pCMB) [21], and by $HgCl_2$ (Balkanski, private communication), whereas other sulfhydryl reagents, *N*-ethylmaleimide and iodoacetamide, have no effect [21]. We have observed the same pattern for inhibition of DBDS binding to band 3 in red cell ghosts (see Table II). Cysteine reverses both the inhibition of water transport in intact red cells [21] and the inhibition of DBDS binding to band 3 in ghosts as shown in Table II. The similar effects of the

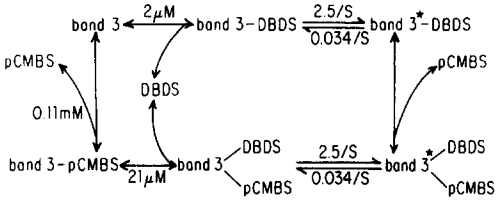

Fig. 5. Mechanism for binding of pCMBS and DBDS to band 3.

TABLE II

EFFECTS OF SULFHYDRYL REAGENTS ON DBDS BINDING TO GHOSTS

IAM, iodoacetamide; NEM, *N*-ethylmaleimide.

Conditions	Time constant
Ghosts + 1 μM DBDS [a]	1.9 ± 0.1
+ 1 mM IAM	2.1 ± 0.1
+ 0.5 mM pCMB	5.0 ± 0.3
+ 0.5 mM pCMBS	4.8 ± 0.3
+ 0.05 mM $HgCl_2$	4.0 ± 0.3
Reversibility and NEM experiments	
Ghosts + 1 μM DBDS [b]	1.3 ± 0.3
+ NEM treatment [b]	1.6 ± 0.1
+ NEM + 2 mM pCMBS [b]	4.0 ± 0.2
+ NEM + 2 mM pCMBS + 5 mM cysteine [c]	1.2 ± 0.4

[a] Solutions were prepared in 28.5 mM sodium citrate (pH 7.4), at a ghost concentration of 0.04 mg/ml ghost protein. Ghosts were *N*-ethylmaleimide treated for these experiments, as described under Methods.

[b] This set of experiments was performed in 28.5 mM sodium citrate/5 mM NaCl (pH 7.4) so that the chloride concentration was kept constant when cysteine·HCl was added.

[c] 28.5 mM sodium citrate (pH 7.4).

organic mercurial sulfhydryl reagents pCMBS and pCMB on DBDS binding to ghosts, as well as the reversibility of the effect by cysteine suggest that a sulfhydryl bond is formed when pCMBS binds to ghost membranes.

Band 3 contains six sulfhydryl groups [13,14]; five of these react with both *N*-ethylmaleimide and pCMBS [18], as discussed in Methods. The sixth sulfhydryl reacts only with pCMBS, and it has been located on the 15 kDa transmembrane fragment near the anion transport inhibitor site (Rothstein and Ramjeesingh, [16]). Since the ghosts used in our experiments were treated with *N*-ethylmaleimide, the pCMBS effect on the DBDS binding can be attributed to this sixth sulfhydryl group. The sixth sulfhydryl group also appears to be responsible for the pCMBS inhibition of water transport in intact red cells [9].

Acknowledgements

We wish to thank Dr. Alfred Pandiscio for his technical advice and Mr. Bernard Corrow for constructing the apparatus used to perform the stopped-flow measurements. Supported in part by USPHS grants HL14820 and GM00782. This work was done during the tenure of a research fellowship (MFL) from the American Heart Association, Western Mass. Division number 13-401-812.

References

1 Knauf, P.A. (1979) Current Topics in Membranes and Transport, Vol. 12 (Bronner, F. and Kleinzeller, A., eds.), pp. 249–263, Academic Press, New York
2 Lukacovic, M.F., Feinstein, M.B., Sha'afi, R.I. and Perrie, S. (1981) Biochemistry 20, 3145–3151
3 Rao, A., Martin, P., Reithmeier, R.A.F. and Cantley, L.C. (1979) Biochemistry 18, 4505–4516
4 Verkman, A.S., Dix, J.A. and Solomon, A.K. (1983) J. Gen. Physiol. 81, 421–449
5 Dix, J.A., Verkman, A.S. and Solomon, A.K. and Cantley, L.C. (1979) Nature 282, 520–522
6 Brown, P.A., Feinstein, M.B. and Sha'afi, R.I. (1975) Nature 254, 523–525
7 Macey, R.I. and Farmer, R.E.L. (1970) Biochim. Biophys. Acta 211, 104–106
8 Van Steveninck, J., Weed, R.I. and Rothstein, A. (1965) J. Gen. Physiol. 48, 617–632
9 Solomon, A.K., Chasan, B., Dix, J.A., Lukacovic, M.F., Toon, M.R. and Verkman, A.S. (1983) Ann. N.Y. Acad. Sci. 414, 97–124
10 Kotaki, A., Naoi, M. and Yagi, K. (1971) Biochim. Biophys. Acta 229, 547–556
11 Dodge, J.T., Mitchell, C. and Hanahan, D.J. (1963) Arch. Biochem. Biophys. 100, 119–130
12 Lowry, O.H., Rosebrough, N.J., Farr, A.L. and Randall, R.J. (1951) J. Biol. Chem. 193, 265–275
13 Steck, T.L., Koziarz, J.J., Singh, M.K., Reddy, G. and Kohler, H. (1978) Biochemistry 17, 1216–1222
14 Ramjeesingh, M., Gaarn, A. and Rothstein, A. (1980) Biochim. Biophys. Acta 559, 127–139
15 Rao, A. (1979) J. Biol. Chem. 254, 3503–3511
16 Rothstein, A. and Ramjeesingh, M. (1982) Phil. Trans. Roy. Soc. Lond. B 299, 497–507
17 Rao, A. and Reithmeier, R.A.F. (1979) J. Biol. Chem. 254, 6144–6150
18 Rao, A. (1978) Ph. D. Thesis, Harvard University, Cambridge, MA
19 Segel, I.H. (1975) Enzyme Kinetics, Wiley, New York
20 Czerlinski, G.H. (1966) Chemical Relaxation, Marcel Dekker, New York
21 Sha'afi, R.I. and Feinstein, M.B. (1977) Adv. Exp. Med. Biol. 84, 67–80